

# Induction of Synaptic Long-Term Potentiation After Opioid Withdrawal

Ruth Drdla,\* Matthias Gassner,\* Ewald Gingl, Jürgen Sandkühler†

$\mu$ -Opioid receptor (MOR) agonists represent the gold standard for the treatment of severe pain but may paradoxically also enhance pain sensitivity, that is, lead to opioid-induced hyperalgesia (OIH). We show that abrupt withdrawal from MOR agonists induces long-term potentiation (LTP) at the first synapse in pain pathways. Induction of opioid withdrawal LTP requires postsynaptic activation of heterotrimeric guanine nucleotide-binding proteins and *N*-methyl-D-aspartate receptors and a rise of postsynaptic calcium concentrations. In contrast, the acute depression by opioids is induced presynaptically at these synapses. Withdrawal LTP can be prevented by tapered withdrawal and shares pharmacology and signal transduction pathways with OIH. These findings provide a previously unrecognized target to selectively combat pro-nociceptive effects of opioids without compromising opioid analgesia.

Opioids are widely used by pain patients and by addicts. Abrupt withdrawal from acute opioid application may lead to opioid-induced hyperalgesia (OIH) that is also a key feature of the highly aversive withdrawal syndrome after prolonged opioid consumption (1). Several mechanisms have been proposed to underlie OIH (2–7). It has been suggested that

opioid-induced and injury-induced hyperalgesia share underlying mechanisms (8, 9). A synaptic model of injury-induced hyperalgesia is the long-term potentiation (LTP) at synapses between nociceptive C fibers and neurons in superficial spinal dorsal horn (10, 11). It is an intriguing but as yet unproven hypothesis that opioids may not only modify (12, 13) but also induce synaptic

plasticity (13). We tested this hypothesis directly. We used a slice preparation from rat lumbar spinal dorsal horn with long dorsal roots attached. Whole-cell recordings were made from lamina I neurons with monosynaptic excitatory input from C fibers (14). Bath application of the MOR agonist D(-)-2-amino-5-phosphonopentanoic acid (DAMGO) for 15 min induced a rapid, dose-dependent depression of C fiber-evoked excitatory postsynaptic currents (EPSCs) in all neurons tested without evidence of acute tolerance [inhibition was to  $40 \pm 7\%$  (SEM) at 2 min of application and to  $39 \pm 7\%$  at 15 min; Fig. 1, A and B]. Upon washout of DAMGO, responses became potentiated to  $165 \pm 17\%$  of control 15 min after washout in 10 out of 14 neurons (Fig. 1, A and B). This opioid withdrawal LTP remained undiminished for the remaining recording periods of up to 100 min.

High doses of spinal morphine may lead to nonspecific OIH that is not mediated by opioid

Department of Neurophysiology, Center for Brain Research, Medical University of Vienna, Spitalgasse 4, 1090 Vienna, Austria.

\*These authors contributed equally to this work.

†To whom correspondence should be addressed. E-mail: juergen.sandkuehler@meduniwien.ac.at

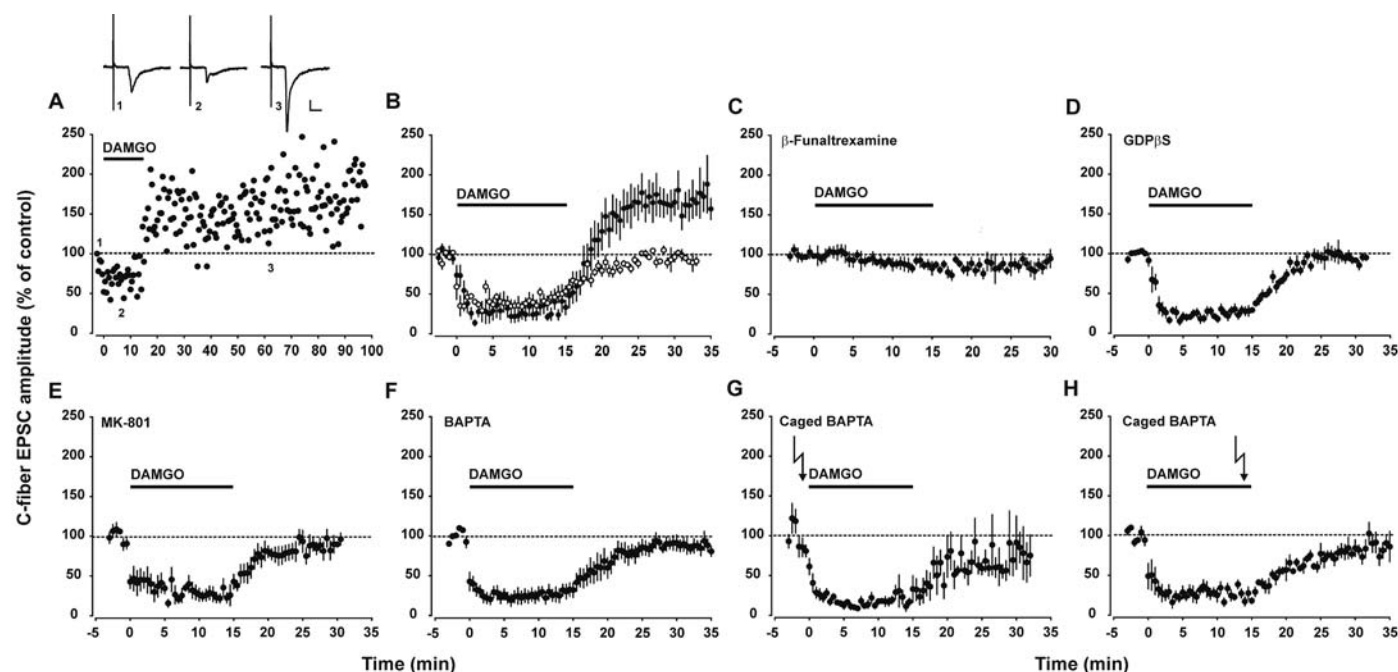


**Fig. 1.** LTP induction at synapses of afferent C fibers in vitro by acute application of MOR agonist DAMGO involves postsynaptic G protein coupling and NMDA receptor-dependent  $\text{Ca}^{2+}$  signaling. (A) Opioid withdrawal LTP in a spinal cord lamina I neuron. DAMGO ( $0.5 \mu\text{M}$ ) was bath-applied for 15 min beginning at time 0 (black horizontal bar in all graphs). Amplitudes of individual C fiber-evoked EPSCs were normalized to predrug values and plotted versus time. The dotted lines in this and all other graphs indicate normalized EPSC amplitudes before DAMGO application. Insets show individual EPSC traces recorded at the indicated time points; calibration bars indicate 10 ms and 20 pA. (B) Average time courses of 10 neurons where DAMGO induced an acute synaptic depression ( $P = 0.001$ ) and LTP upon washout ( $P = 0.001$ ; solid circles) and four neurons in which DAMGO produced an acute depression only ( $P = 1$ ; open circles). Error bars indicate 1 SEM. (C) Bath application of MOR

antagonist  $\beta$ -funaltrexamine ( $25 \mu\text{M}$ ) blocked both acute depression and LTP induction in all five neurons tested ( $P = 0.011$ ). (D) Blocking postsynaptic G protein coupling with GDP- $\beta$ -S added to the pipette solution ( $0.5 \text{ mM}$ ) blocked LTP induction in all five neurons tested without affecting acute synaptic depression ( $P = 0.011$ ). (E) Blocking postsynaptic NMDA receptors with MK-801 added to the pipette solution abolished LTP induction in all five neurons tested ( $P = 0.011$ ). (F) Preventing postsynaptic rise in  $[\text{Ca}^{2+}]_i$  by  $\text{Ca}^{2+}$  chelator BAPTA added to the pipette solution fully blocked LTP induction but not acute synaptic depression in six out of seven neurons ( $P = 0.024$ ). (G) Caged BAPTA was added to the pipette solution and released by flash photolysis (flash symbol) 1 min before DAMGO application. This blocked LTP induction in all five neurons tested ( $P = 0.011$ ). (H) As in (G) but with flash photolysis 1 min before washout of DAMGO ( $P = 0.011$ ).

receptors (15, 16). We excluded any nonspecific effects by showing that acute depression and withdrawal LTP were both abolished by blockade

of opioid receptors with naloxone (fig. S1) and by the MOR selective antagonist  $\beta$ -funtaltrexamine (Fig. 1C). Any contribution of  $\gamma$ -aminobutyric acid

type A ( $GABA_A$ ) or glycine receptors, for example by disinhibition of synaptic strength (17, 18) or block of LTP at inhibitory synapses (12), can be

**Fig. 2.** Opioids induce  $Ca^{2+}$  rise in superficial spinal dorsal horn neurons in vitro during application and/or during washout. In transverse slices from lumbar spinal dorsal horn, lamina I neurons were filled with fura-2 pentapotassium salt through the patch pipette to measure  $Ca^{2+}$  gradients during bath application of DAMGO (horizontal bars) and upon washout. From a total of 35 superficial spinal dorsal horn neurons tested, 11 responded with an elevation of  $Ca^{2+}$  during DAMGO application (A), 8 neurons responded upon washout (B), 7 neurons displayed dual responses (C), and 9 neurons did not show any rise in  $Ca^{2+}$  (D). Solid lines represent mean values, and gray areas, one SEM.

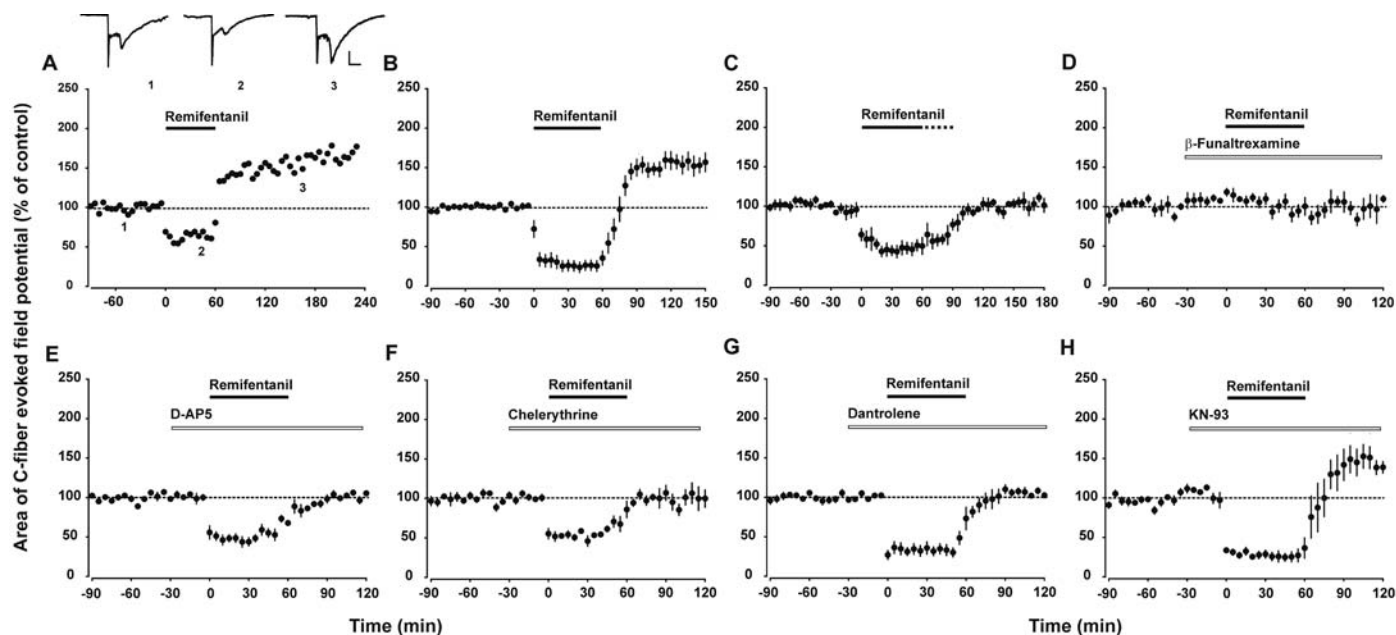
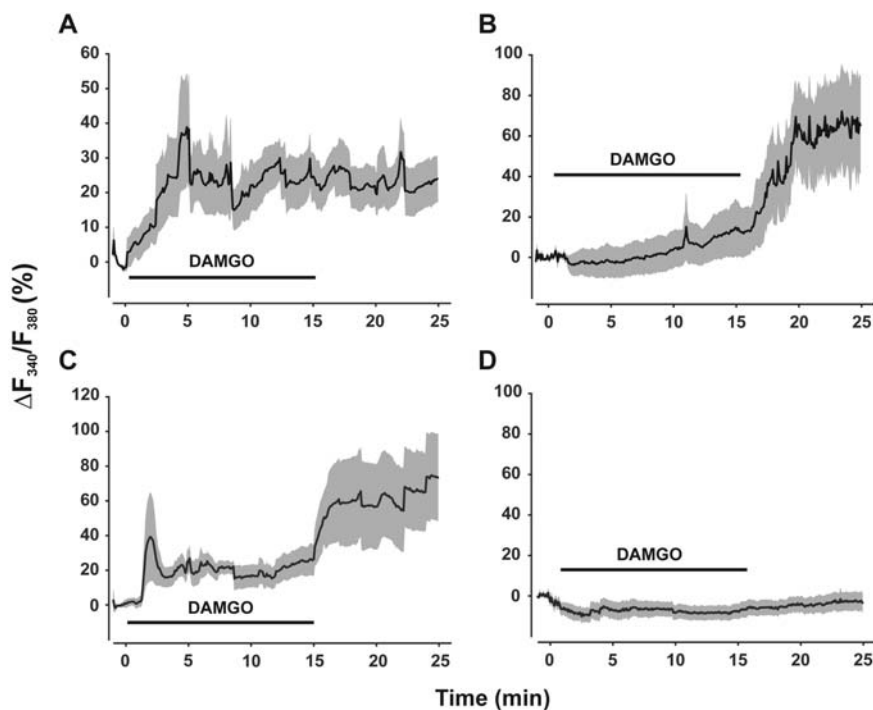


**Fig. 3.** Intravenous infusions of ultrashort-acting MOR agonist remifentanyl induce LTP at C fiber synapses in vivo that involves activation of spinal NMDA receptors and PKC but not CaMKII. (A) Time course of the curve of individual C fiber-evoked field potentials in one rat. Values were normalized to predrug values (dotted line) and plotted versus time. In this and in all other graphs, remifentanyl was injected as a bolus ( $30 \mu\text{g} \cdot \text{kg}^{-1}$ ) followed by an infusion ( $450 \mu\text{g} \cdot \text{kg}^{-1} \cdot \text{hour}^{-1}$  for 1 hour, black horizontal bars). Insets show individual traces of field potentials recorded at indicated time points. Calibration bars, 100 ms and 0.5 mV. (B) Averaged time course of C fiber-evoked field potentials recorded from 14 animals where withdrawal induced LTP ( $P = 0.001$ ). Error bars indicate 1 SEM. (C) Tapered withdrawal (dotted line) from remifentanyl over a period of 30 min prevented the potentiation of C fiber-evoked field

potentials in all five animals tested ( $P = 0.001$ ). (D) Spinal superfusion with  $\beta$ -funtaltrexamine ( $250 \mu\text{M}$ , open horizontal bar) abolished acute depression and withdrawal LTP in all five animals tested ( $P = 0.001$ ). (E) Topical application of NMDA receptor blocker D-AP5 ( $100 \mu\text{M}$ , open horizontal bar) blocked LTP induction ( $P = 0.001$ ) but not acute synaptic depression by remifentanyl ( $P = 1$ ). (F) Spinal application of PKC inhibitor chelerythrine chloride ( $800 \mu\text{M}$ , open bar) blocked LTP induction ( $P = 0.001$ ) but not synaptic depression by DAMGO ( $P = 1$ ). (G) Spinal application of the ryanodine receptor blocker dantrolene ( $500 \mu\text{M}$ , open bar) blocked LTP induction ( $P = 0.001$ ) but not acute depression by remifentanyl ( $P = 1$ ). (H) In contrast, spinal application of CaMKII blocker KN-93 at a concentration ( $400 \mu\text{M}$ , open bar) that blocks activity-dependent LTP in this in vivo model (23) failed to affect opioid withdrawal LTP ( $P = 1$ ).

ruled out because experiments were done in the presence of bicuculline and strychnine.

Blockade of postsynaptic heterotrimeric guanine nucleotide-binding proteins (G proteins) with guanosine 5'-O-(2'-thiodiphosphate) (GDP- $\beta$ -S) included in the pipette solution abolished opioid withdrawal LTP without affecting the acute depression of synaptic strength in C fibers (Fig. 1D). This suggests that withdrawal LTP requires postsynaptic G protein signaling. In contrast, the depressant effect of opioids is induced presynaptically at these synapses.

OIH and activity-dependent forms of LTP at C fiber synapses require activation of *N*-methyl-D-aspartate (NMDA) receptors (8, 10). Blockade of postsynaptic NMDA receptors by MK-801 added to the pipette solution fully blocked opioid withdrawal LTP without affecting acute synaptic depression by DAMGO (Fig. 1E). Adding the  $\text{Ca}^{2+}$  chelator BAPTA [1,2-bis(2-aminophenoxy) ethane-*N,N,N',N'*-tetraacetic acid] to the pipette solution had the same effect (Fig. 1F). OIH may develop during continuous chronic application of opioids or upon their withdrawal. The time point when opioids elevate intracellular calcium ion concentrations ( $[\text{Ca}^{2+}]_i$ ) to cause LTP is, however, not known. We found that in individual lamina I neurons  $[\text{Ca}^{2+}]_i$  may rise during acute opioid application (Fig. 2A), upon washout (Fig. 2B), or both (Fig. 2C). We next asked which of these different types of  $\text{Ca}^{2+}$  rise is essential for the induction of withdrawal LTP. We used a caged form of BAPTA to chelate  $\text{Ca}^{2+}$  ions in the postsynaptic neurons at defined time points by flash photolysis. When BAPTA was uncaged before DAMGO application, withdrawal LTP was prevented (Fig. 1G), confirming the previous experiment with BAPTA added to the pipette solution (Fig. 1F). Flash photolysis directly before the washout of DAMGO also fully blocked withdrawal LTP (Fig. 1H), indicating that a rise in postsynaptic  $[\text{Ca}^{2+}]_i$  upon opioid withdrawal is essential for the induction of withdrawal LTP.

To evaluate whether opioid withdrawal LTP exists in the spinal cord of living animals with descending and segmental inhibitory systems intact, we next recorded C fiber-evoked field potentials in the superficial spinal dorsal horn of deeply anaesthetized adult rats (11). We used the ultrashort-acting MOR agonist remifentanyl, which induces OIH in humans and in rodents. Intravenous injections of remifentanyl caused a rapid depression of C fiber-evoked field potentials to  $30 \pm 8\%$  within 5 min and to  $33 \pm 8\%$  at 60 min, suggesting that no acute tolerance developed. Upon abrupt termination of the infusion, responses were potentiated in 14 out of 16 animals tested (Fig. 3, A and B). Mean potentiation was to  $149 \pm 1\%$  of control ( $n = 14$ ) at 120 to 150 min after the infusion and remained undiminished throughout the recording period of up to 4 hours (Fig. 3A). Boli only or shorter infusions (30 min) also led to withdrawal LTP but with lower incidence (fig. S2, A and B). Opioid withdrawal LTP was prevented when opioid infusion was tapered off over a period of 30 min (Fig. 3C). Application of vehicle only had no effect (fig. S2D). After intravenous remifentanyl injection, opioid receptors in spinal cord mediated both the acute synaptic depression and the withdrawal LTP because spinal application of naloxone (fig. S2C) or  $\beta$ -funaltrexamine (Fig. 3D) blocked both effects. Blockade of NMDA receptors by spinal superfusion with the NMDA receptor antagonist [D-Ala<sup>2</sup>, N-MePhe<sup>4</sup>, Gly-ol]-enkephalin (D-AP5) also abolished withdrawal LTP in vivo but had no effect on the acute depression by systemic remifentanyl (Fig. 3E). OIH apparently involves activation of protein kinase C (PKC) (19–21). Consistently, spinal application of PKC blocker chelerythrine abolished induction of withdrawal LTP without affecting the acute depression of synaptic strength (Fig. 3F).

Activity-dependent forms of LTP at C fiber synapses involve  $\text{Ca}^{2+}$  release from intracellular ryanodine receptor-sensitive  $\text{Ca}^{2+}$  stores and activation of calcium-calmodulin-dependent pro-

tein kinase II (CaMKII) (11, 22, 23). Blockade of ryanodine receptors by spinal superfusions with dantrolene blocked withdrawal LTP (Fig. 3G), whereas spinal application of CaMKII blocker KN-93 was ineffective (Fig. 3H). Thus, opioid withdrawal LTP requires a rise in postsynaptic  $\text{Ca}^{2+}$ , likely fueled by  $\text{Ca}^{2+}$  influx through NMDA receptor channels and by the release from intracellular stores. Interestingly, the CaMKII blocker had no effect, either on acute depression or on potentiation. Signaling pathways between opioid withdrawal LTP and activity-dependent forms of LTP thus overlap only partially.

It is not known whether opioids may also raise  $\text{Ca}^{2+}$  levels in spinal neurons in vivo. To test this directly, we used in vivo two-photon laser-scanning microscopy and assessed  $\text{Ca}^{2+}$  gradients in superficial dorsal horn neurons before, during, and after intravenous application of remifentanyl. Of the 31 lamina I neurons tested, 15 responded with an elevation of  $\text{Ca}^{2+}$  concentration to the application of the opioid. In 6 neurons  $\text{Ca}^{2+}$  levels rose during drug application (Fig. 4A). In 9 other neurons,  $\text{Ca}^{2+}$  concentration remained constant during infusions but rose upon withdrawal from the opioid (Fig. 4B). One might thus speculate that these two patterns of  $\text{Ca}^{2+}$  rise consistently found in vivo and in vitro and involving distinct neuronal populations in superficial spinal dorsal horn may contribute to different forms of OIH. One that develops during continuous opioid application might contribute to opioid tolerance (8, 20, 24, 25), and another one that may be part of the opioid withdrawal syndrome (21).

We have identified an activity-independent form of LTP that is induced by withdrawal from acute application of MOR agonists. This opioid withdrawal LTP shares signal transduction pathways with OIH. Opioid withdrawal- and activity-dependent forms of LTP (11, 22) at C fiber synapses require activation of NMDA receptors, rise in postsynaptic  $\text{Ca}^{2+}$ , and activation of PKC. NMDA receptors have a PKC phosphorylation site, and phosphorylation removes the voltage-sensitive  $\text{Mg}^{2+}$  block (26). This may lead to NMDA receptor activation and  $\text{Ca}^{2+}$  influx at or near the resting membrane potential in the absence of any presynaptic activity, possibly by glial cell-derived glutamate (27) or elevated glutamate levels during opioid withdrawal (28).

OIH typically includes enhanced responsiveness to C fiber-mediated noxious mechanical and thermal stimuli (1). Collectively the published and present data suggest that opioid withdrawal LTP at synapses of nociceptive C fibers is a mechanism of OIH. We found that withdrawal LTP can be prevented by a tapered withdrawal regime and that it is mechanistically and spatially distinct from opioid-induced synaptic depression. This encourages hopes that OIH may be targeted specifically without interfering with powerful opioid analgesia.

#### References and Notes

1. M. S. Angst, J. D. Clark, *Anesthesiology* **104**, 570 (2006).
2. F. Simonin et al., *Proc. Natl. Acad. Sci. U.S.A.* **103**, 466 (2006).

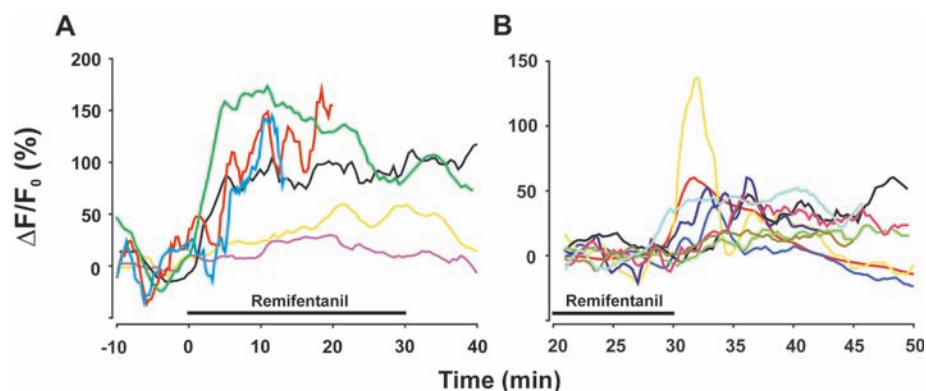


**Fig. 4.** In vivo imaging of  $\text{Ca}^{2+}$  gradients in superficial spinal dorsal horn neurons during application and upon washout of an opioid. A cardiopulmonary bypass was used to improve mechanical stability (14).  $\text{Ca}^{2+}$  gradients of a total of 31 neurons were monitored. (A) Six neurons responded with elevated  $\text{Ca}^{2+}$  levels during opioid application ( $P < 0.001$ ). (B) Nine other neurons displayed  $\text{Ca}^{2+}$  rise upon washout ( $P < 0.001$ ). Sixteen neurons did not respond with a significant change in  $[\text{Ca}^{2+}]_i$  to opioid application. Each neuron is represented by a different color.

3. H.-Y. Wang, E. Friedman, M. C. Olmstead, L. H. Burns, *Neuroscience* **135**, 247 (2005).
4. J. P. Fry, A. Herz, W. Zieglgänsberger, *Br. J. Pharmacol.* **68**, 585 (1980).
5. C. H. Brown, J. A. Russell, *Stress* **7**, 97 (2004).
6. L. R. Gardell *et al.*, *J. Neurosci.* **22**, 6747 (2002).
7. T. W. Vanderah *et al.*, *J. Neurosci.* **21**, 279 (2001).
8. D. J. Mayer, J. Mao, J. Holt, D. D. Price, *Proc. Natl. Acad. Sci. U.S.A.* **96**, 7731 (1999).
9. A. Vardanyan *et al.*, *J. Pain* **10**, 243 (2008).
10. J. Sandkühler, *Physiol. Rev.* **89**, 707 (2009).
11. H. Ikeda *et al.*, *Science* **312**, 1659 (2006).
12. F. S. Nugent, E. C. Penick, J. A. Kauer, *Nature* **446**, 1086 (2007).
13. J. T. Williams, M. J. Christie, O. Manzoni, *Physiol. Rev.* **81**, 299 (2001).
14. Materials and methods are available as supporting material on Science Online.
15. C. J. Woolf, *Brain Res.* **209**, 491 (1981).
16. T. L. Yaksh, G. J. Harty, B. M. Onofrio, *Anesthesiology* **64**, 590 (1986).
17. W. Zieglgänsberger, E. D. French, G. R. Siggins, F. E. Bloom, *Science* **205**, 415 (1979).
18. C. W. Vaughan, S. L. Ingram, M. A. Connor, M. J. Christie, *Nature* **390**, 611 (1997).
19. L. Chen, L.-Y. Huang, *Neuron* **7**, 319 (1991).
20. J. Mao, D. D. Price, D. J. Mayer, *J. Neurosci.* **14**, 2301 (1994).
21. S. M. Sweitzer *et al.*, *Pain* **110**, 281 (2004).
22. H. Ikeda, B. Heinke, R. Ruscheweyh, J. Sandkühler, *Science* **299**, 1237 (2003).
23. R. Drdla, J. Sandkühler, *Mol. Pain* **4**, 18 (2008).
24. L. P. Vera-Portocarrero *et al.*, *Pain* **129**, 35 (2007).
25. B. L. Kieffer, C. J. Evans, *Cell* **108**, 587 (2002).
26. L. Chen, L.-Y. Huang, *Nature* **356**, 521 (1992).
27. P. Sah, S. Hestrin, R. A. Nicoll, *Science* **246**, 815 (1989).
28. K. H. Jhamandas, M. Marsala, T. Ibuki, T. L. Yaksh, *J. Neurosci.* **16**, 2758 (1996).
29. Supported by grant no. P18129-B02 from the Austrian Science Fund (FWF).

#### Supporting Online Material

[www.sciencemag.org/cgi/content/full/325/5937/207/DC1](http://www.sciencemag.org/cgi/content/full/325/5937/207/DC1)

Materials and Methods

Figs. S1 and S2

References

2 February 2009; accepted 12 May 2009

10.1126/science.1171759

# Induction of Synaptic Long-Term Potentiation After Opioid Withdrawal

Ruth Drdla, Matthias Gassner, Ewald Gingl, Jürgen Sandkühler

## Materials and Methods

All experiments were performed in accordance with the European Community's Council directives (86/609/ECC) and were approved by the Austrian Federal Ministry for Education, Science and Culture.

## Spinal cord slice preparation

Under deep isoflurane anesthesia, the lumbar spinal cord was removed from young rats (aged 17 to 25 days). Transverse slices (about 500  $\mu\text{m}$  thick) with long dorsal roots (10-15 mm) attached were cut using a vibrating microslicer. Slices were incubated in a solution kept at 33°C containing (in mM): NaCl, 95; KCl, 1.8;  $\text{KH}_2\text{PO}_4$ , 1.2;  $\text{CaCl}_2$ , 0.5;  $\text{MgSO}_4$ , 7;  $\text{NaHCO}_3$ , 26; glucose, 15; sucrose, 50; pH was 7.4, osmolarity 310-320  $\text{mosmol}\cdot\text{l}^{-1}$ , and oxygenated with 95%  $\text{O}_2$  and 5%  $\text{CO}_2$ . A single slice was then placed in the recording chamber and continuously superfused with oxygenated recording solution at a rate of 3-4  $\text{ml}\cdot\text{min}^{-1}$ . The recording solution was identical to the incubation solution except for (in mM): NaCl, 127;  $\text{CaCl}_2$ , 2.4;  $\text{MgSO}_4$ , 1.3 and sucrose 0, and was kept at 33 °C with an inline solution heater.

## Electrophysiological recordings in vitro

Neurons were visualized with infrared optics (SI). Only neurons lying within a distance of maximally 20  $\mu\text{m}$  from the dorsal white/grey matter border were considered as being lamina I neurons and used for the experiments. All recordings were made in the whole-cell patch-clamp configuration at a holding potential of -70 mV using an Axopatch 200B patch-clamp amplifier and the pCLAMP 9 acquisition software. Signals were low-pass filtered at 2-10 kHz, sampled at 10 kHz. Patch pipettes (impedance 2-5 M $\Omega$ ) from borosilicate glass were pulled on a horizontal puller and filled with

internal solution (mM): potassium gluconate 120, KCl 20,  $\text{MgCl}_2$  2,  $\text{Na}_2\text{ATP}$  2, NaGTP 0.5, HEPES 20, EGTA 0.5, pH 7.28 with KOH, measured osmolarity 300  $\text{mosm}\cdot\text{l}^{-1}$ . For some experiments, patch pipettes were filled with a  $\text{K}^+$  free solution composed of (in mM):  $\text{CsMeSO}_3$ , 120; TEA-Cl, 20;  $\text{MgCl}_2$ , 2; HEPES, 10; EGTA, 10;  $\text{Na}_2\text{ATP}$ , 2; and GDP $\beta\text{S}$ , 500  $\mu\text{M}$ . The potassium free GDP $\beta\text{S}$ -solution was used to prevent postsynaptic opioid receptor mediated effects (S2, S3). For blocking intracellular  $\text{Ca}^{2+}$  the  $\text{Ca}^{2+}$ -chelator BAPTA (20 mM) was added to the pipette solution consisting of (in mM): potassium gluconate 100, KCl 20,  $\text{MgCl}_2$  4,  $\text{Na}_2\text{ATP}$  2, NaGTP 0.5, HEPES 10, pH 7.28 with KOH, measured osmolarity 300  $\text{mosm}\cdot\text{l}^{-1}$ . For blocking postsynaptic NMDA-receptors MK-801 (10  $\mu\text{M}$ ) was added to the standard internal solution.

Dorsal root afferents were stimulated through a suction electrode with an isolated current stimulator. After determination of the threshold to elicit an EPSC, test pulses of 0.1 ms were given at intervals of 30 s. Intensity of test stimulation ranged from 3 to 5 mA. Evoked EPSCs were classified as C-fiber-evoked when the calculated conduction velocity was below 0.5  $\text{m}\cdot\text{s}^{-1}$ . Monosynaptic C-fiber input was identified by the absence of failures in response to 10 stimuli applied at 2 Hz to the dorsal roots and a jitter in response latencies of less than 2 ms.

In some experiments electrophysiology was combined with UV-flash photolysis. For flash photolysis Diazo-2 tetrapotassium salt (2 mM) was added to the pipette solution composed of (in mM): potassium gluconate 120, KCl 20,  $\text{MgCl}_2$  2,  $\text{Na}_2\text{ATP}$  2, NaGTP 0.5, HEPES 20, pH 7.28 with KOH, measured osmolarity 300  $\text{mosm}\cdot\text{l}^{-1}$ . Uncaging was performed with a UV-

flash (Mercury Lamp 100 W) at 360 nm for 1 sec.

#### **In vitro Ca<sup>2+</sup> imaging of spinal cord neurons**

Fluorometric measurements of free cytosolic Ca<sup>2+</sup> concentrations of single lamina I dorsal horn neurons were performed by loading the cells in the recording chamber via a patch pipette by replacing EGTA in the standard pipette solution with the cell-impermeant dye fura-2 pentapotassium salt (250  $\mu$ M). Slices were continuously superfused with recording solution containing bicuculline and strychnine. Experiments were performed at 33°C. Neurons were clamped at -70 mV in the whole cell patch-clamp configuration. For Ca<sup>2+</sup> imaging, cells were illuminated with a monochromator and images were taken with a cooled CCD camera. Paired exposures to 340 and 380 nm were obtained at a frame rate of 0.2 Hz. In all experiments, one drug effect was tested per slice.

#### **Animal surgery for in vivo experiments**

Experiments were performed on adult male Sprague Dawley rats (200-250 g for electrophysiology and 90-120 g body weight for imaging). Isoflurane (4 vol %) in two thirds N<sub>2</sub>O and one third O<sub>2</sub> was initially applied through an anesthesia mask to induce anesthesia. Animals were then intubated using a 16 G venous cannula and mechanically ventilated at a rate of 75 strokes·min<sup>-1</sup> and a tidal volume of 4-6 ml. Anesthesia was maintained using 1.5 vol % isoflurane.

Core temperature was kept at 37.5  $\pm$  2°C with a feedback controlled heating blanket. Deep surgical level of anesthesia was verified by stable mean arterial blood pressure. The right femoral vein and artery were cannulated to allow i.v. infusions and for monitoring arterial blood pressure, respectively. Muscle relaxation was achieved by 2  $\mu$ g·kg<sup>-1</sup>·h<sup>-1</sup> pancuronium bromide i.v.. For cardiopulmonary bypass (see below) in- and outflow a carotid artery and a jugular vein were cannulated. During anesthesia, animals continuously received i.v. solution (58% Ringer solution, 30% HAES, 8% glucose and 4% sodium bicarbonate, 2 ml·h<sup>-1</sup>) for stabilization of blood pressure (mean arterial blood pressure 120  $\pm$  10 mmHg), blood-glucose (mean 100  $\pm$  10 mg·dl<sup>-1</sup>) and base excess (-1.5  $\pm$  0.8 mmol·l<sup>-1</sup>). Following cannulation, the left sciatic nerve was dissected free for bipolar electrical stimulation with a silver hook electrode. The lumbar segments L4 and L5 were exposed by

laminectomy. The dura mater was incised and reflected.

A portable stereotactic frame with two adjustable brackets for vertebral column fixation was custom made to fit on the microscope stage for imaging experiments (see below). The stereotactic frame permitted a prone position of the animal for cardiopulmonary bypass and for electrophysiological recordings in vivo. An agarose pool was formed around the exposed spinal segments and filled with artificial cerebrospinal fluid. A bipolar hook stimulation electrode was fixed directly onto the steel base plate for stimulation of sciatic nerve fibers. At the end of each electrophysiological experiment animals were decapitated in deep anesthesia, the spinal cord was removed and cryo-fixed for detection of a rhodamine B spot at the recording site under a fluorescence microscope. Only those experiments were taken into further analysis where the recording site was in laminae I or II.

#### **Electrophysiological recordings in vivo**

Electrophysiological recordings were performed as described elsewhere (S4). Briefly, C-fiber-evoked field potentials were recorded with glass electrodes (impedance 2-3 M $\Omega$ ) from laminae I and II of the spinal cord dorsal horn in response to stimulation of sciatic nerve fibers. The pipette solution consisted of (in mM) NaCl 135, KCl 5.4, CaCl<sub>2</sub> 1.8, HEPES 10 and MgCl<sub>2</sub> 1, and in addition 0.2 % rhodamine B. At the end of each electrophysiological experiment, pressure was applied to the electrode (300 mbar, 1 min) for marking the recording site with rhodamine B. Electrodes were driven by a microstepping motor. Recordings were made with an ISO-DAM-amplifier using a band width filter of 0.1 – 1000 Hz. Signals were monitored on a digital oscilloscope and digitized by an A/D converter. Afferent input from the hindpaw was identified by mechanical stimulation of the foot while acoustically evaluating the evoked responses with an audio monitor. Test stimuli were delivered to the sciatic nerve and consisted of single pulses of 0.5 ms at intensity of 25 V given every 5 minutes using an electrical stimulator. To explore the signal transduction pathways involved, specific blockers were topically applied to the spinal cord dorsum (S5).

#### **Cardiopulmonary bypass for in vivo Ca<sup>2+</sup> imaging experiments**

The extracorporeal circuit consisted of a venous reservoir, a membrane oxygenator and a heat

exchanger. Blood was drained from the right atrium via the jugular vein catheter into a 5 ml reservoir, which was closed for generation of a slight vacuum to support venous outflow. The venous reservoir was connected to a roller pump equipped with a 12 cm long silicone tube with a 2 mm internal diameter. A heat exchanger was located between the roller pump and the oxygenator. The membrane oxygenator made of micro porous polypropylene fibers was custom built. Cardiopulmonary bypass was conducted during imaging at a flow rate of  $150 \text{ ml}\cdot\text{kg}^{-1}\cdot\text{min}^{-1}$ , which is similar to normal cardiac output in the rat (S6). Thereby sufficient blood gas exchange was provided throughout the whole cardiopulmonary bypass period. Blood pressure and arterial blood gas analyses were thereby kept within physiological limits.

#### **In vivo dye loading of spinal cord neurons**

Freshly made  $250 \mu\text{M}$  Oregon Green BAPTA-1 AM (solved in 0.5 % Pluronic 127 in buffer) was pressure injected into superficial laminae of the exposed spinal cord. The proper injection area was identified by field potential recordings which were evoked by electrical stimulation of sciatic nerve fibers (see below). Following 30 min de-esterification of the dye, the animal was placed under the 2-photon laser-scanning microscope for imaging. To eliminate movement artefacts from respiration, a cardiopulmonary bypass was used during imaging.

#### **In vivo $\text{Ca}^{2+}$ imaging of spinal cord neurons**

Imaging was performed on a 2-photon laser scanning microscope consisting of a DM LFS A microscope and a femtosecond Ti-sapphire laser operating at 90 MHz repeat frequency, 140 fs pulse width and a wavelength range of 705 - 980 nm. Excitation light was focused by an x40 water immersion objective (0.8 NA). The excitation wavelength was set to 750 nm for Oregon Green BAPTA. The average power delivered to the spinal cord surface was less than 200 mW. Scanning and imaging acquisition were controlled with confocal software. Emitted light was collected by a non-descanned detector for monitoring the calcium dye Oregon Green BAPTA (525/50). Long-term fluorescent measurements were achieved by repeatedly bidirectional scanning of a region of  $512 \times 128$  pixels at a time interval of 300 ms – 6 s and heart beat triggered. Fast fluorescent scanning at a region of  $128 \times 64$  or  $256 \times 128$  pixels was done at a time interval 92 – 184 ms.

#### **Drugs**

For in vitro electrophysiology and in vitro  $\text{Ca}^{2+}$  imaging experiments, drugs were applied to the bath solution at known concentrations. Drugs used were bicuculline ( $10 \mu\text{M}$ ), strychnine ( $10 \mu\text{M}$ ), the selective  $\mu$ -opioid receptor agonist [D-Ala<sup>2</sup>, N-Me-Phe<sup>4</sup>, Gly-ol]-enkephalin (DAMGO,  $500 \text{ nM}$ ) and  $\beta$ -funaltrexamine ( $25 \mu\text{M}$ ).

For in vivo recording pancuronium bromide was given as an i.v. infusion ( $2 \text{ mg}\cdot\text{kg}^{-1}\cdot\text{h}^{-1}$ ). Remifentanyl was dissolved in sterile NaCl. For a tapered withdrawal remifentanyl infusion was reduced from  $450 \mu\text{g}\cdot\text{kg}^{-1}\cdot\text{h}^{-1}$  to zero in 15 equal steps at 2 min intervals beginning 60 min after onset of infusion (Fig. 3C).  $\beta$ -Funaltrexamine was applied topically onto the spinal cord surface ( $250 \mu\text{M}$ ). The competitive N-methyl D-aspartate (NMDA) receptor antagonist D(-)-2-Amino-5-phosphonopentanoic acid (D-AP5,  $100 \mu\text{M}$ ) was dissolved in 0.9% NaCl. The protein kinase C (PKC) blocker chelerythrine chloride ( $800 \mu\text{M}$ ) was dissolved in ddH<sub>2</sub>O. The  $\text{Ca}^{2+}$ -calmodulin dependent kinase II (CaMKII) blocker 2-[N-(2-hydroxyethyl)]-N-(4-methoxybenzenesulfonyl)]amino-N-(4-chlorocinnamyl)-N-methylbenzylamine (KN-93,  $400 \mu\text{M}$ ) and the ryanodine receptor blocker dantrolene ( $500 \mu\text{M}$ ) were dissolved in DMSO. All drugs were further dissolved in artificial cerebrospinal fluid to obtain the desired concentrations as indicated in the figure legend and applied directly onto the spinal cord dorsum (S5).

#### **Data analysis and statistics**

C-fiber-evoked EPSCs were analyzed offline using Clampfit 9. Synaptic strength was quantified by measuring the peak amplitude of monosynaptic EPSCs. Amplitudes were used to quantify synaptic strength as they were not affected by occasional action potential discharges. The mean amplitude of 6 EPSCs evoked by test stimuli prior to opioid application served as control. Statistical comparison was assessed using SigmaStat 3.1. Data were tested for normality (Kolmogorov-Smirnov Test), and then a one way repeated measures analysis of variance (One Way RM-ANOVA) was performed for each neuron to test for potentiation. Effects of drugs were tested using the Fisher Exact test.

The area under the curve of C-fiber-evoked field potentials was determined offline using the software Clampfit 9. Amplitudes and areas under the curve of C-fiber-evoked field

potentials changed in parallel in all experiments. For data analysis the area under the curve was used as amplitudes displayed higher variability (coefficients of variation of up to 200%; on average 25%). The mean area under the curve of 18 consecutive field potentials prior opioid application served as control. Responses were normalized for each rat. Data were tested for normality, and then a One Way RM-ANOVA was performed to compare the different experimental protocols and treatments. ANOVA was corrected by the Bonferroni adjustment. Effects of drugs were tested using the Fisher Exact test. A p-value < 0.05 was considered statistically significant. Values are expressed as mean  $\pm$  standard error of mean (SEM).

In vivo  $\text{Ca}^{2+}$  transients were measured using 512 x 128 pixels scans at a time interval of 6 s. Images were processed and quantified with ImageJ 1.37c. Fluorescence was averaged over cell body areas and expressed as relative

fluorescence changes ( $F/F_0$ ) after subtraction of background fluorescence.

The 10 min periods prior to drug application or washout of the opioid served as controls. Data were tested for normality and changes in fluorescence intensity were assessed using the Rank-Sum test. Values are plotted as running averages with a sampling proportion of 0.05.

For in vitro  $\text{Ca}^{2+}$  imaging, the ratio of exposures to 340 and 380 nm light (F340/F380) was calculated off-line to assess the relative change in  $\text{Ca}^{2+}$ -concentration without conversion to absolute concentration values. For single cell measuring, a region of interest was placed in the centre of the cell soma. Data were normalized to the period 1 min prior drug application. To assess changes in fluorescence intensity due to drug application a One Way RM-ANOVA was performed. ANOVA was corrected by the Bonferroni adjustment. Data are expressed as mean  $\pm$  standard error of mean (SEM).

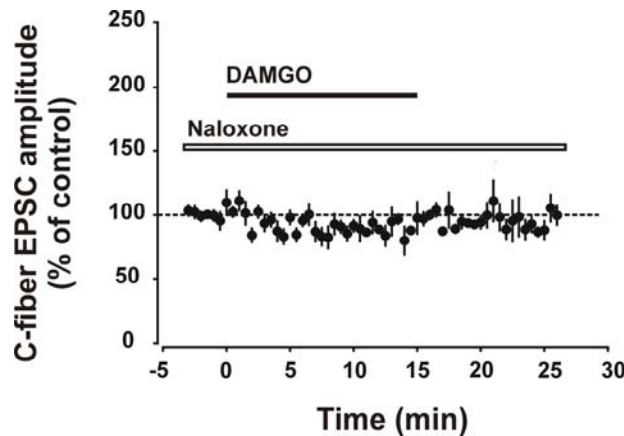


**Fig S1.** Opioid-induced acute depression and opioid withdrawal LTP are blocked by the opioid-receptor antagonist naloxone. The average time course of C-fiber evoked EPSCs in lamina I neurons is shown. Bath application of naloxone (10  $\mu\text{M}$ ) fully blocked both, acute depression and LTP induction in all 5 neurons tested ( $p = 0.011$ ).



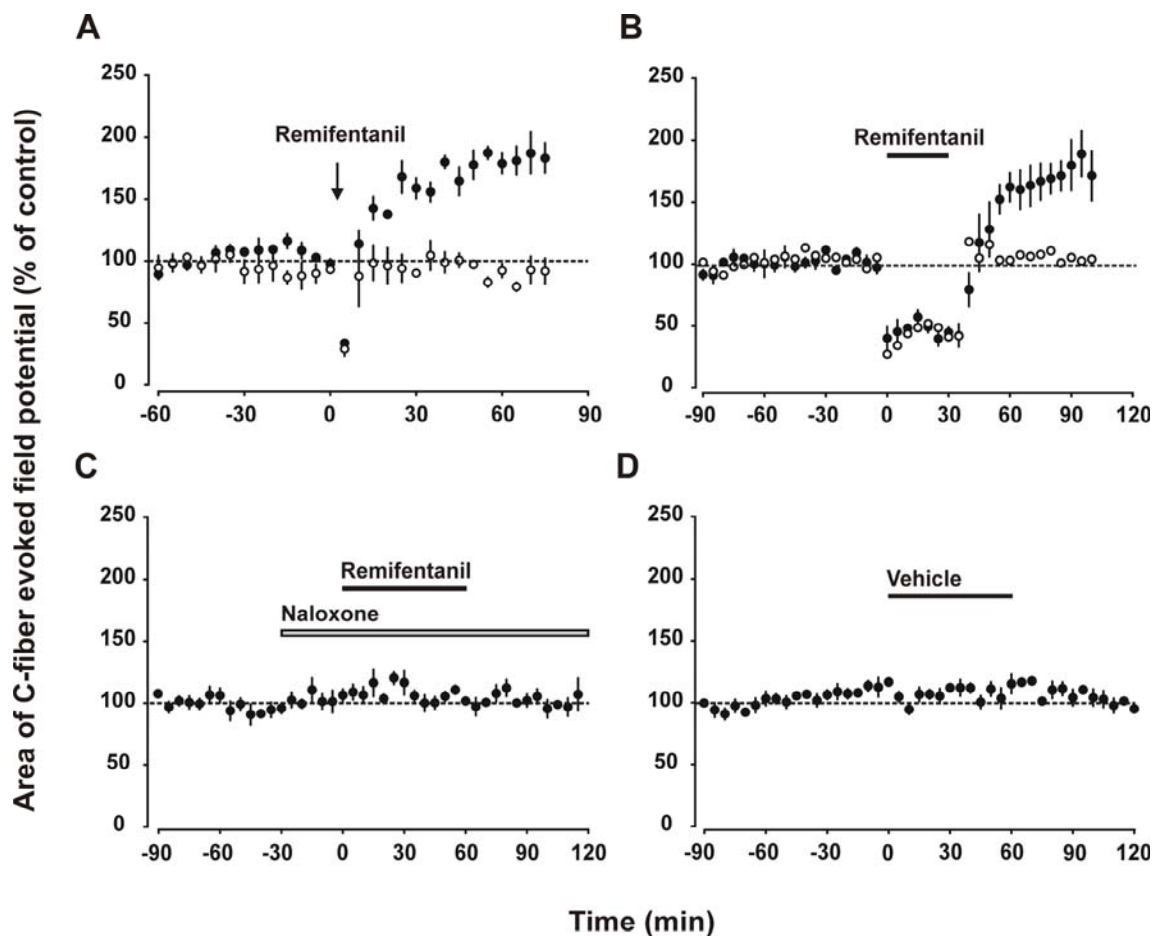


**Fig S2.** Intravenous infusion of remifentanyl induces LTP at C-fiber synapses *in vivo*. In all graphs, mean time course of area under the curve of C-fiber evoked field potentials are shown. Values were normalized to pre-drug values (dotted line) and plotted against time (min). **(A)** Bolus injection ( $30 \mu\text{g}\cdot\text{kg}^{-1}$ , downward arrow) of remifentanyl led to potentiation of C-fiber evoked field potentials upon wash-out of the opioid in 3 animals (closed circles,  $p = 0.001$ ) whereas it had no effect in 2 other animals tested (open circles,  $p = 0.375$ ). **(B)** Remifentanyl injected as a bolus followed by an infusion ( $450 \mu\text{g}\cdot\text{kg}^{-1}\cdot\text{h}^{-1}$ , black horizontal bar) for 30 min induced LTP in 4 animals tested (closed circles,  $p = 0.004$ ). No effect was observed in one animal (open circles,  $p = 0.266$ ). **(C)** Spinal superfusion with naloxone ( $10 \mu\text{M}$ , open horizontal bar) abolished acute depression and opioid withdrawal LTP in all 5 animals that received a one hour remifentanyl infusion ( $p = 0.001$ ). **(D)** The commercially available formula of remifentanyl contains glycine as a vehicle. Intravenous injection of glycine in the appropriate concentration (S7, S8) for one hour (closed bar) had no effect in any of the 4 animals tested ( $p = 0.001$ ).

## References

- S1. H.-U. Dodt, M. Eder, A. Frick, W. Zieglgänsberger, *Science* **286**, 110 (1999).
- S2. M. Ikoma, T. Kohno, H. Baba, *Anesthesiology* **107**, 807 (2007).
- S3. T. Ataka, E. Kumamoto, K. Shimoji, M. Yoshimura, *Pain* **86**, 273 (2000).
- S4. H. Ikeda *et al.*, *Science* **312**, 1659 (2006).
- S5. H. Beck, H. Schröck, J. Sandkühler, *J. Neurosci. Methods* **58**, 193 (1995).
- S6. W. R. Chenitz, B. A. Nevins, N. K. Hollenberg, *Am. J. Physiol.* **231**, 961 (1976).
- S7. K. Hahnenkamp *et al.*, *Anesthesiology* **100**, 1531 (2004).
- S8. E. Guntz *et al.*, *Anesthesiology* **102**, 1235 (2005).